# Eco-Driving Operation of Connected Vehicle With V2I Communication Among Multiple Signalized Intersections

**Qingfeng Lin**
*Is with the School of Transportation Science and Engineering, Beihang University, Beijing. Email: linqf@buaa.edu.cn*

**Shengbo Eben Li***
*Is with the State Key Lab of Automotive Safety and Energy, Department of Automotive Engineering, Tsinghua University, Beijing. Email: lisb04@gmail.com*

**Shaobing Xu**
*Is with the Department of Mechanical Engineering, University of Michigan, Ann Arbor. Email: xushao@umich.edu*

**Xuejin Du**
*Is with the School of Transportation Science and Engineering, Beihang University, Beijing. Email: 15201316042@163.com*

**Diange Yang**
*Is with the State Key Lab of Automotive Safety and Energy, Department of Automotive Engineering, Tsinghua University, Beijing. Email: ydg@tsinghua.edu.cn*

**Keqiang Li**
*Is with the State Key Lab of Automotive Safety and Energy, Department of Automotive Engineering, Tsinghua University, Beijing. Email: likq@tsinghua.edu.cn*

xxxxxxx

*Digital Object Identifier 10.1109/MITS.2020.3014113*
*Date of current version: 17 September 2020*

*Corresponding author


1939-1390/20©2020IEEE

***Abstract*—**Eco-driving through multiple intersections has significant fuel benefit for road transportation. Most existing studies assume that vehicles travel at a constant speed between intersections, which naturally leads to large errors in fuel prediction and trajectory planning. This article focuses on eco-driving operation through multiple signalized intersections considering more realistic powertrain dynamics, which directly contain the engine and the transmission as well as aerodynamic drag, rolling resistance, and so on. This feature enables explicit descriptions of dynamic behaviors and fuel characteristics in acceleration, deceleration, and constant speed driving. An open-loop optimal control problem (OCP) is formulated to minimize fuel consumption between two red-signalized intersections, and the two- or three-stage operation rules are then proposed to approximate its optimal solution. The eco-driving of passing multiple intersections is then numerically solved by combining the two- or three-stage driving rule and the Dijkstra algorithm. This method can consider the acceleration and deceleration processes at each intersection and achieve improved fuel economy.

Connected vehicle technologies have the ability to significantly improve traffic mobility and safety, enabling information exchange between the vehicle and the infrastructure (V2I) through wireless communication. Apart from reducing unimpaired crashes, it also combines with automated vehicles to fulfill more functions, such as emergency braking, remote diagnostics, and eco-driving [1].

Two different approaches generally have been adopted to apply experienced driving skills to eco-driving projects. First, fuel-saving skills were taught through driver education, fuel-gauge feedback, and real-time monitoring [2]–[5]. Second, fuel-saving tips were implemented in advanced driver assistance systems, such as cruise control, adaptive cruise control, or even autonomous driving systems. A firm understanding of fuel-saving strategies is critical for both approaches. One way to acquire fuel-saving strategies is to parse the general rule from a large quantity of driving data collected from experienced drivers. A host of eco-driving projects have employed this method and generated a variety of eco-driving tips, such as accelerating smoothly and eliminating excessive idling [6]–[8]. These tips are qualitative and cannot ensure optimality in any sense; they can be used for driver education but are not ready for implementation in vehicle control. Another way to obtain fuel-saving strategies is to extract fuel-saving rules directly from the powertrain dynamics and engine fuel characteristics. For example, Li and Peng [9] identified an optimal fuel operating strategy of car-following scenarios. It was found that the optimal strategy of the following vehicle changes from partial pulse-and-gliding operation to regular pulse-and-gliding operation, and finally to constant speed operation as the leading vehicle's speed increases. Li et al. [10], [11] further examined the periodic operation for internal combustion engine-based vehicles in free-driving scenarios. By using the π-test, Li et al. [11] found the fuel-saving mechanism is essentially caused by singular arcs due to the S-shaped engine fueling rate.

Another typical scenario is driving through multiple signalized intersections, for which the past researches that target its eco-driving strategies usually use two types of approaches. One approach is based on empirical rules (such as reducing idle time at intersections) and uses many traffic simulations to verify its effectiveness. It can be easily implemented, but the results cannot guarantee optimality. For example, Sato et al. [12] focused on the strategy of early upshifting transmission gears, and the experimental results demonstrated that this strategy could achieve a reduction of 15–34% in $CO_2$ emissions.

The second approach is based on optimization methodologies, such as the Dijkstra algorithm or dynamic programing (DP), and converts the problem of economically passing through intersections into an open-loop optimal control problem that aims to minimize fuel consumption. It can numerically calculate the accurate vehicle trajectory at signalized intersections; however, the heavy computation load poses challenges in practical deployment.

For instance, Thomas and Voulgaris [13] employed the Dijkstra algorithm to compute the optimal path. It delivers the optimal speed trajectory, but the assumption that the vehicle travels between two intersections at a constant speed is not realistic because the vehicle would accelerate or decelerate during the traveling process [13]. De Nunzio et al. [14] found energy optimal velocity profiles for a vehicle in urban traffic by proposing a preliminary velocity pruning algorithm to identify a feasible region under city speed limits, and then a velocity trajectory advised by Dijkstra algorithm allows the vehicle to pass through the signalized intersections without stopping. Kamalanathsharma and Rakha [15] used a multistage DP to compute a fuel-optimal vehicle trajectory by receiving traffic signal information, and the results of simulations suggested that it can save fuel for multiple intersections in the range of 19% and travel time in the range of 32%. Kamalanathsharma and Rakha [16] used a moving horizon dynamic programming approach to optimize the trajectory of a vehicle approach-

ing an intersection. Rakha and Kamalanathsharma [17] proposed a DP-based fuel-optimization strategy to generate fuel-efficient vehicle trajectories in the vicinity of traffic signalized intersections by controlling the vehicle variable limiting speed to minimize fuel consumption. This work was further extended to integrate queue estimation [18].

Zeng and Wang [19] presented the optimal speed planning solution based on DP for a vehicle running on a given route with multiple stop signs, traffic lights, turns and curved segments, roads of different grades and speed limits. Schuricht et al. [20] proposed a predictive driver assistance system based on the transmission of traffic light controller information to the approaching vehicle and uses the distance to a virtual stop line and time to a queue-cleared intersection to calculate an energy-efficient speed profile. Xia et al. [21] considered dynamic eco-driving in an arterial corridor by providing signal phase and timing (SPaT) information of traffic lights to the vehicle so that it could adjust its velocity with the goal of minimizing fuel consumption, thereby reducing individual vehicle fuel consumption by about 10–15%. Sun et al. [22] developed a dynamic eco-driving speed guidance strategy (DESGS), which adopted a rolling horizon optimization and a DP approach to generate the most fuel-minimized speed profile for a vehicle approaching signalized intersections. It was found that the fuel consumption could be reduced by approximately 25% for vehicles with DESGS as compared to vehicles without speed guidance [22]. A speed advisory system (SAS) for reducing idling at red lights has been proposed [23], and results showed that the fuel consumption of both SAS-equipped vehicles and other conventional vehicles in a fleet decreased and that the fleet fuel economy improved with the increment of the percentage of SAS-equipped vehicles. In addition, Tang et al. [24] developed an extended car-following model accounting for remaining green time to study the driving behavior, fuel consumption, and emissions of each vehicle during the whole process of running across a signalized intersection.

On the whole, these methods rely on the optimization method and use vehicle connectivity to acquire traffic SPaT. To enhance computational efficiency, they use either simple vehicle dynamics or simple fuel consumption models. For instance, the simple fuel consumption model cannot embody real fuel consumption, as it ignores the powertrain dynamics and is just a function of speed and/or acceleration. Thus, both the simplified fuel consumption model and the vehicle longitudinal dynamics model will result in a high error in vehicle speed trajectory prediction for multiple intersections.

Some recent studies on eco-driving have considered both accurate vehicle dynamics and powertrain operation in scenarios such as car-following or cruising control. However, in eco-driving design, vehicle powertrain dynamics are often neglected to simplify the problem formulation. For example, Jin et al. [32] proposed a power-only–based longitudinal control algorithm for connected eco-driving to pass through one single signalized intersection. Ozatay et al. [25] investigated an analytical solution to the fuel-minimized problem when facing one single traffic light and assumes that the vehicle travels only at a constant acceleration or deceleration, which is less realistic.

This article explores the eco-driving operation through multiple signalized intersections by considering more realistic powertrain dynamics. The vehicle dynamic model directly includes the engine and the transmission as well as aerodynamic drag and rolling resistance. This allows the model to describe dynamic behaviors and fuel characteristics in acceleration, deceleration, and constant speed driving. The open-loop optimal control problem of a vehicle passing through a single section (bounded by two red-signalized intersections) is first formulated. Then we propose a two- or three-stage operation rule to approximate its optimal solution, and then apply them from a single section to multiple intersections. Finally, the Dijkstra algorithm is used to search the optimal parameters of the proposed operation rule for minimizing fuel consumption.

## Eco-Driving Operation Between Two Intersections

Here we focus on a single section to explore the basic eco-driving operations, i.e., the driving rules minimizing the fuel consumption when passing through two red-signalized intersections. These strategies will then be extended from two intersections to multiple intersections in the next section.

### *Fuel Minimum Optimal Control Problem for a Single Section*

The studied vehicle used an internal combustion engine (ICE) and a continuously variable transmission (CVT). The ICE was a four-cylinder 2.0-L gasoline engine. To achieve the optimal operation, the eco-driving task was formulated as an optimal control problem (OCP) [26]–[27]:

$$C = \min J = \int_0^{t_f} Q_s \mathrm{d}t,$$

subject to

$$\begin{aligned}
\begin{pmatrix} \dot{s} \\ \dot{v} \end{pmatrix} &= \begin{pmatrix} 0 & 1 \\ 0 & -\dfrac{C_A v^2 + Mfg}{\delta M v} \end{pmatrix} \begin{pmatrix} s \\ v \end{pmatrix} + \begin{pmatrix} 0 \\ \dfrac{\eta_T}{\delta M v} \end{pmatrix} P_e, \\
T_{eco}(w_{eco}) &= k_{eco}(w_{eco} - b)^\gamma, \\
i_g &= \frac{\pi r_w}{cvi_0} \cdot w_{eco}, \\
Q_s &= a_0 + a_1 P_e + a_2 P_e^2 + k_e \left( \frac{\mathrm{d}P_e}{\mathrm{d}t} \right)^2 \\
P_{emin} &\le P_e \le P_{emax}, \\
i_{gmin} &\le i_g \le i_{gmax} \\
0 &\le v \le v_{max},
\end{aligned} \tag{1}$$

$$\boldsymbol{x}(0) = (0 \;\; 0)^T,$$
$$\boldsymbol{x}(t_f) = (S_f \;\; 0)^T,$$

where $Q_s$ is the instantaneous fuel injection rate, and $t_f$ is the terminal time, which is a free variable (depending on the vehicle speed). The state vector is $\boldsymbol{x} = (s, v)^T$; the control input is the engine power $P_e$; $s$ is the travel distance between two intersections; $v$ is the speed; $T_{eco}$ is the engine torque; $w_{eco}$ is the engine speed; and $i_g$ is the CVT gear ratio. The other parameters are listed in Table 1.

Due to the nonlinearity in the cost function and vehicle dynamics, the OCP is difficult to solve analytically. Here we will adopt the Legendre pseudospectral (LPS) method to convert the OCP to a nonlinear programming problem and solve it using the mature toolbox SNOPT [27]–[31]. The order $N$ of the Legendre polynomials is not fixed and can be set to roughly 20–80; we used 30 in this article. The initial values of the resultant optimization problem are set to 0.

### *Optimization Results*

An example of eco-driving between two red-signalized intersections with different distance is presented in Figure 1. The speed limit is set to 30 m/s. The results show that the vehicle travels under either an acceleration–deceleration process (called the two-stage mode) or an acceleration–cruising–deceleration process (called the three-stage mode). More specifically, for a certain speed limit, a turning point exists where the eco-driving operation changes from the two-stage to the three-stage mode. Here we summarize [26], [27]:

- Under an arbitrary speed limit, the eco-driving operation is that the vehicle travels under the two-stage mode if the distance between the two red-signalized intersections is less than a certain distance.
- Under an arbitrary speed limit, the eco-driving operation switches from the two-stage to the three-stage mode when the distance between the two red-signalized intersections is greater than a certain distance threshold.

We also found that the eco-driving operations were similar when comparing the various speed trajectories, especially in the acceleration/deceleration process, i.e., similar acceleration profiles even if the distance between two intersections changes significantly (see Figure 1).

### *The Two- or Three-Stage Operation Rule*

The two- or three-stage operation rule is proposed as the quasi-optimal method for a fast speed trajectory. The idea of the three-stage operation rule is illustrated in Figure 2. Some facts are listed here [26], [27]:

- The constant cruising speed ($v_c$) is determined by the economical speed ($v_{eco}$; the cruising speed at which the car achieves the highest fuel economy), calculated from

**Table 1. The key parameters of vehicle dynamics.**

| Parameters | Meaning | Value |
|---|---|---|
| $C_A$ | $C_A = 0.5 C_D \rho_a A_v$ | 0.43 |
| $C_D$ | The aerodynamic drag coefficient | 0.316 |
| $\rho_a$ | The air density | 1.2258 |
| $A_v$ | The frontal area of the vehicle | 2.22 |
| $M$ | The vehicle mass | 1,600 kg |
| $f$ | The coefficient of the rolling resistance | 0.028 |
| $\delta$ | The lumped rational inertial coefficient | 1.2 |
| $g$ | The gravity coefficient | 9.8 m/s$^2$ |
| $\eta_T$ | The mechanical efficiency of the powertrain system | 0.9 |
| $\gamma$ | The fitting parameters | 1/3 |
| $k_{eco}$ | The fitting parameters | 11.133 g/s |
| $b$ | The fitting parameters | 1,000 |
| $i_0$ | The gear ratio of the final drive | 3.863 |
| $r_w$ | The wheel radius | 0.307 m |
| $c$ | The fitting parameters | 30 |
| $k_e$ | The correction coefficient for transient operations | $8 \times 10^{-4}$ |
| $a_0$ | The fitting parameters | 3.048 |
| $a_1$ | The fitting parameters | 0.0905 |
| $a_2$ | The fitting parameters | 0.00148 |
| $P_{emin}$ | The minimum value of the engine power | 0 kW |
| $P_{emax}$ | The maximum value of the engine power | 126 kW |
| $i_{gmin}$ | The minimum value of the gear ratio | 0.5 |
| $i_{gmax}$ | The maximum value of the gear ratio | 2.8 |

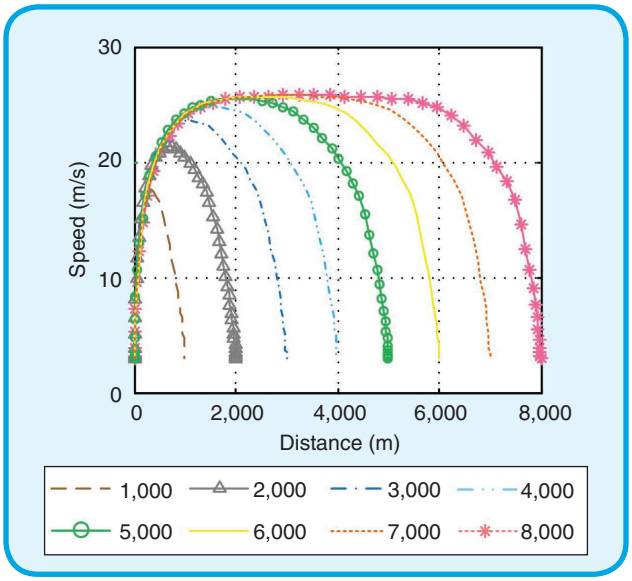


**FIG 1** The vehicle speed profiles under different travel distances solved by the Legendre pseudospectral method.

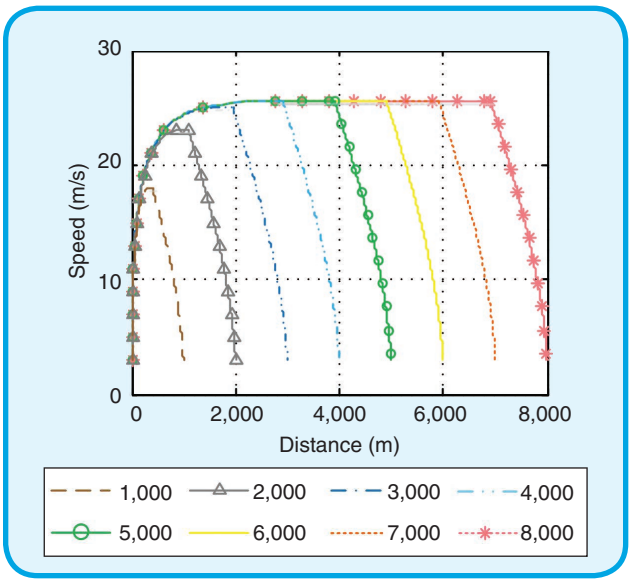


**FIG 2** The vehicle speed profiles under different distances solved by the quasi-optimal strategy.

engine map and vehicle parameters) and the speed limit ($v_{\max}$) according to (2):

$$v_c = \min\{v_{\text{eco}}, v_{\max}\}. \tag{2}$$

- Because the initial speed ($v_{a0} = 0$ m/s) and final speed ($v_{\text{af}} = v_c$) in the acceleration stage are determined, the acceleration process can be acquired according to the economical acceleration profiles, determined by the maximum acceleration and acceleration.
- Similarly, since the initial speed ($v_{d0} = v_c$) and the final speed ($v_{\text{df}} = 0$ m/s) of the deceleration stage are determined, the deceleration process can also be acquired according to the economical deceleration profiles, which is the free-coasting operation. Note that by following the known economical acceleration/deceleration profiles, the global optimality is lost, but it is a near-optimal and computationally efficient strategy.
- Excluding the acceleration/deceleration stages, the remaining distance is traversed in the constant speed stage. The final speed ($v_{\text{af}}$) of the acceleration stage and the initial speed ($v_{d0}$) of the deceleration stage are equal to $v_c$, i.e.,

$$v_c = v_{\text{af}} = v_{d0}. \tag{3}$$

With the previous steps, the whole three-stage operation rule is formed, whose total fuel consumption is calculated as follows:

$$J_T = J_a + J_c + J_d = q_s(v_{\text{af}}, 0) S_a / v_{\text{af}} + \int_0^{v_{\text{af}}} E_\Delta dv + \int_{t_{\text{af}}}^{t_{\text{cf}}} q_s(P_e) dt + \int_{t_{\text{cf}}}^{t_{\text{df}}} q_s(P_e) dt, \tag{4}$$

where $v_{\text{af}}$ is the final speed of the acceleration stage; $t_{\text{af}}$, $t_{\text{cf}}$, and $t_{\text{df}}$ are the final times of the acceleration stage, the constant-speed stage, and the deceleration stage, respectively; $J_a$, $J_c$, and $J_d$ denote the fuel consumption in the acceleration, constant speed, deceleration stages respectively; $q_s$ is the engine instant fuel injection rate; $v_{\text{af}}$ is the final speed in the acceleration stage; $S_a$ is the traveling distance in acceleration stage; $E_\Delta$ is the equivalent fuel consumption per unit velocity increment; and $q_s$ is the engine instant fuel injection rate.

The two-stage operation rule is a predigestion of the three-stage operation rule performed by removing the constant-speed cruising stage. This rule fits the scenario where the distance between two intersections is less than a threshold, as illustrated in Figure 2.

### *Comparison Between the Optimization Results and the Quasi-Optimal Operations*

To demonstrate the effectiveness of the three-stage operation rule, we carried out simulations of different distances from 1,000 m to 8,000 m and compared the fuel consumption and total computation time of the two methods. If $Q_1$ and $Q_2$ are used to represent the fuel consumption of the three-stage operation rule and the LPS optimization method, respectively, the fuel consumption error [$Q$ error $= (Q_1 - Q_2)/Q_2$] of the three-stage operation rule is less than ±1.5% [22], [23]. For the computing load, using $T_1$ and $T_2$ to represent the computation time of the three-stage operation rule and the LPS optimization method, respectively, we then found that the $T$ ratio ($= T_2/T_1$) belongs to the interval of (200,500), meaning that the three-stage operation rule is about hundreds of times faster than the two-stage rule [26], [27].

## Eco-Driving Operation of a Vehicle Passing Through Multiple Intersections

Figure 3 is a schematic diagram of vehicles passing through multiple intersections. The information between vehicles and traffic signals are transferred using V2I technology. The red line in Figure 3 represents the red light, and the vehicles can pass the intersections at either a green or yellow light.

Because of the dynamically varying signal phase, the three-stage operation rule between two red-signalized intersections proposed in the previous section cannot be applied directly to solve the eco-driving problem of passing through multiple intersections. Therefore, we will split the latter problem into several subproblems.

In this section, we elaborate on how to use the Dijkstra algorithm to acquire fuel-minimized driving of the vehicle passing through multiple intersections. The Dijkstra algorithm can find the shortest path (from an origin node to any other node) in a graph with non-negative edge costs. For implementation, we modeled the eco-driving problem in the following ways:

- A series of feasible speed trajectories with different speed limits (or the cruising speed in the three-stage mode) was generated by presenting the three-stage operation.
- By transferring these feasible paths into an adjacency list, we searched the optimal one among all feasible paths.
- The resultant fuel-minimized driving of passing through multiple intersections was defined as the variable speed driving strategy.

### *Decomposition of Passing the Multiple Intersections*

As an example, Figure 4 demonstrates a road with three signalized intersections. Applying the three/two-stage operation rule designed for two red lights, we can decompose the multiple-intersections problem into several two-intersection subproblems and then search the optimal speed trajectory.

If applying the three-stage operation rule to solve the optimal solution of the multiple-intersections problem, four situations can happen, as demonstrated in Figure 4:

- If all three signal lights are red, the vehicle speed path is ① ② ③.
- If the first signal light is green, and the others are red, the vehicle speed path is ④ ③.
- If the second signal light is green, and the others are red, the speed path is ① ⑤.
- If the first and second signal lights are green, and the third is red, the speed path is ⑥.

### *Vehicle Speed Adjustment of the Three-Stage Operation Rule*

To be more flexible, the two- or three-stage operation rule can be changed slightly to adapt to the dynamic traffic lights, e.g., the initial speed, the final speed, and the constant cruising speed can vary from zero to a minimum value of either economical speed or the road speed limit. By this strategy, we can manipulate the travel time between two intersections.

When the distance between two signalized intersections is fixed, the three-stage modes with different final times are acquired by changing the final speed or the cruising speed of the three-stage operation. This operation transfers the discretization of time into the discretization of the final speed or the constant speed of the three-stage operation. Therefore, the different time nodes can be formed at each signalized intersection, and the different travel routes can be optimized from all feasible candidates.

Figure 5 is a schematic map of the three-stage operation rule with different speed changes. There are four modes in total for the speed adjustment. The first mode and second mode change the initial speed and the final speed, respectively, as illustrated in Figure 5(a) and (b). The third mode changes both the initial speed and the final speed, as illustrated in Figure 5(c). The fourth mode changes only the constant speed, as illustrated in Figure 5(d). With the four modes, although the whole traveling distance is fixed, the travel time can freely change. For example, as demonstrated in Figure 5(a) and (b), the area $A_1 = A_2$, the initial/final speed can be varied from 0 m/s to $v_b/v_f$, and then the whole travel time is decreased.

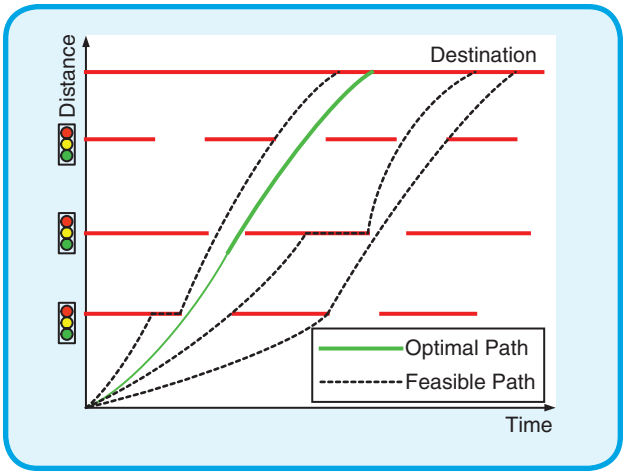


**FIG 3** A schematic fuel-saving path map of a vehicle passing through multiple intersections.

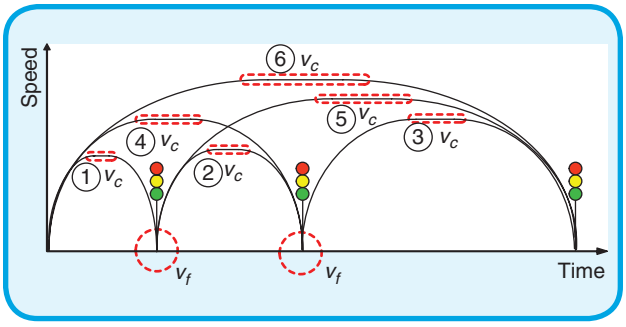


**FIG 4** The entire possible traveling profile for three intersections.

### *Variable Speed Driving Strategy*

#### Feasible Paths for Optimal Fuel Consumption

As illustrated in Figure 6, we here design a directed graph for eco-driving speed design with the known structure of the three-stage rule. Between two adjacent interactions, we can use the three-stage rule with different speed settings and travel time, as presented in the previous section, to generate a lot of speed trajectory candidates. Each trajectory forms a node, depicted as Nodes 2, 3, 4, and 5 in Figure 6. If the time node is in the time duration of a red light, the final speed of the three-stage operation rule is set to 0 m/s (e.g. Node 4). If in the duration of a green light, the final speed is greater than 0 m/s (e.g., Node 2). In addition, the constraint in speed continuity should also be considered and satisfied, e.g., the final

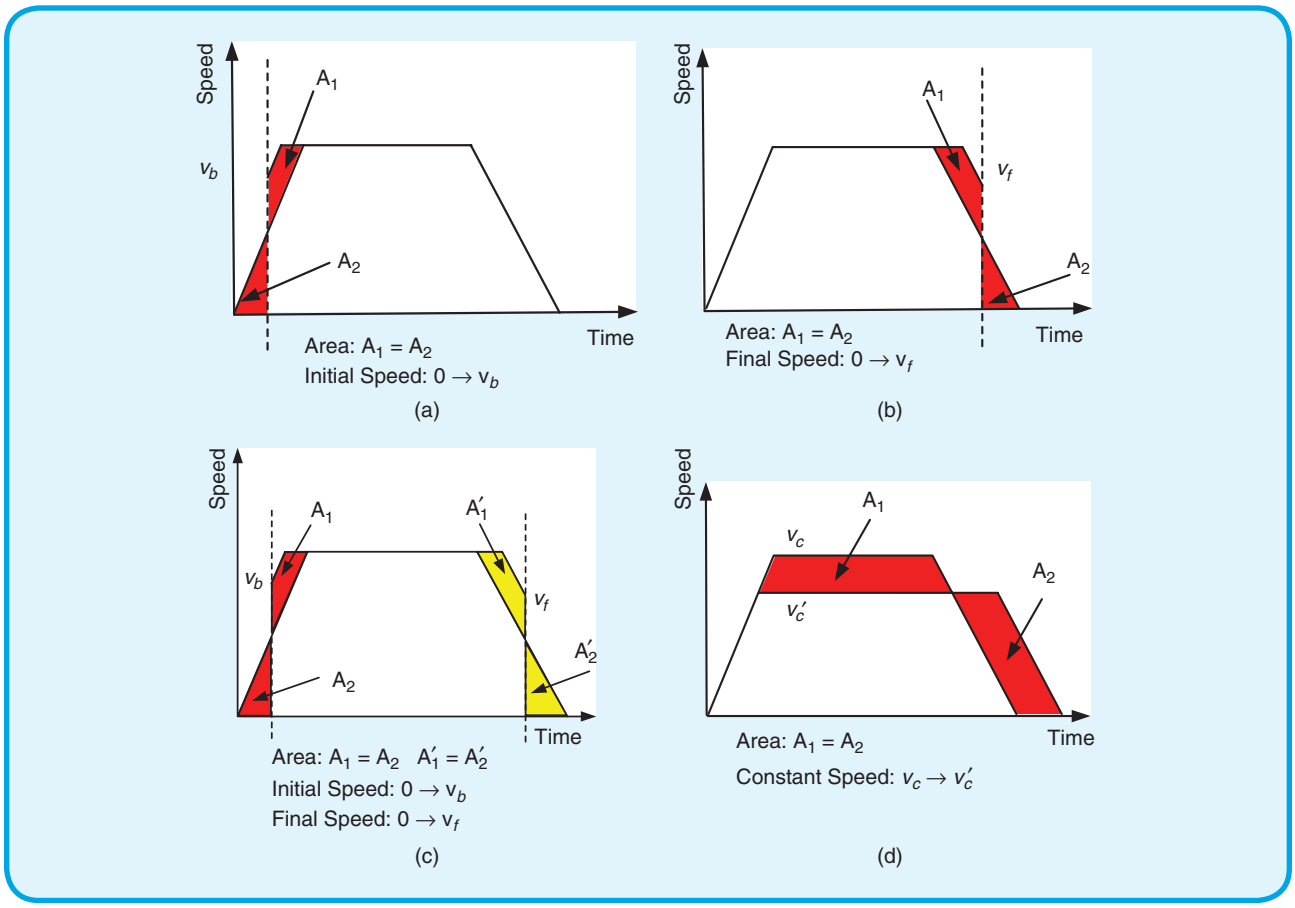


**FIG 5** A schematic map of the three-stage operation rule with different speed changes. (a) The initial speed change mode. (b) The final speed change mode. (c) The initial and final speed change modes. (d) The constant speed change mode.

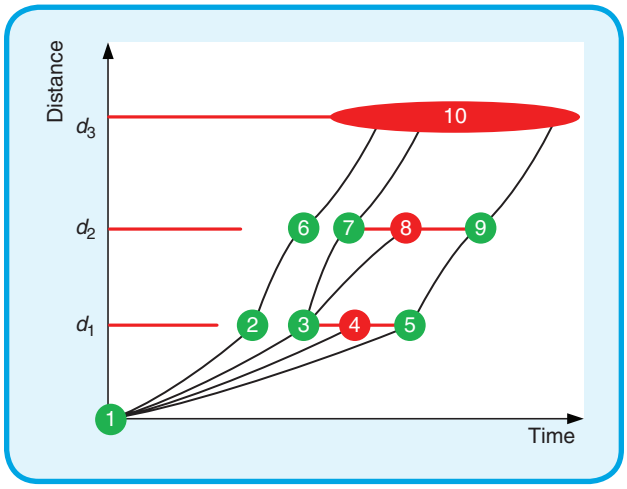


**FIG 6** A schematic map of feasible paths.

speed of the first section (Nodes 1 and 2) should be equal to the initial speed of the next section (Node 2–6). Therefore, a series of feasible paths can be established with the consideration of speed continuity. Figure 6 presents a schematic map of all feasible paths, and $d_1$, $d_2$, and $d_3$ represent the position of three intersections, respectively. The solid red line is the time duration of the red light. The red and green circles denote the arrival points at the intersections. Node 1 is the current vehicle position, and Node 10 is the destination. The solid black line represents only a few feasible paths. Nodes 6, 7, and 9 are connected to Node 10 finally.

### Search for the Eco-Driving Speed Trajectory Based on the Shortest Path Method

Figure 6 could be simplified to a directional graph with weights defined as fuel consumption, as presented in Figure 7. The red nodes represent that the car will meet red lights, and the green nodes represent the time duration of green lights. For the former case, the vehicle needs to wait until the green light is on before launching. For example, Node 4 in Figure 7 can be connected only to Node 5. The fuel consumption between two nodes can be calculated by (4). The fuel consumption of idling can be calculated by (5), such as $q_{45}$ and $q_{89}$:

$$J_{\text{idle}} = \int_{t_i}^{t_j} q_s(P_e)dt = \int_{t_i}^{t_j} a_0 dt, \tag{5}$$

where $J_{\text{idle}}$ is the idle fuel, and $t_i$ and $t_j$ are the initial and final times.

Since the eco-driving problem was transformed into a standard directed graph, we could use the shortest path method to search for the optimal path. In the present study, we applied the Dijkstra algorithm to solve the formulated eco-driving problem. Because of the advantage of storing a sparse matrix, the adjacency list is used to store the relation and weight between different nodes in Figure 7. The adjacency list $C1$ of Figure 7 is given in (6). The first and second rows represent the initial and final node of each path, respectively, and the third row is the fuel consumption between two nodes. For numerical simulations, we can acquire more nodes by discretizing initial speed, final speed, or constant speed more intensively to gain more precise results.

$$C1 = \begin{bmatrix} 1 & 1 & 1 & 1 & 2 & 3 & 3 & 4 & 5 & 6 & 7 & 8 & 9 \\ 2 & 3 & 4 & 5 & 6 & 7 & 8 & 5 & 9 & 10 & 10 & 9 & 10 \\ q_{12} & q_{13} & q_{14} & q_{15} & q_{26} & q_{37} & q_{38} & q_{45} & q_{59} & q_{610} & q_{710} & q_{89} & q_{910} \end{bmatrix}. \quad (6)$$

## Simulation Analysis and Results

Based on the method established in the previous section, the simulations were run with a desktop PC equipped with an Intel Core i5-4570 CPU at 3.20 GHz and 8 GB of RAM. To understand the benefits of the proposed variable speed driving strategy, it is compared with the constant speed driving strategy, which assumes that a vehicle travels only at a constant speed between two intersections [13].

### *Comparison of the Variable Speed and Constant Speed Driving Strategies*

Both urban and suburban environments are designed to compare the variable speed driving strategy with the constant speed driving strategy. For the variable speed driving strategy, the discretized speed interval for final speed and constant speed is 3 m/s in both environments, and the maximum speed (speed limit) in urban and suburban environments is set to 20 and 30 m/s, respectively. For the constant speed driving strategy, the discretized interval of time is 6 s (the gap of two nodes at a certain intersection) in both environments. The distance between intersections and the traffic light phases are listed in Table 2:

Figures 8 and 9 demonstrate the traveling trajectories solved using the two driving strategies in urban and suburban environments. Figures 10 and 11 present their speed profiles. The solid multicolored line represents the variable speed driving strategy, and the solid red line, solid green line, and the solid green line depict the acceleration, constant speed, and deceleration stages, respectively. The dashed black line indicates the constant speed driving strategy. For the variable speed driving strategy, the vehicle idles for 2 s at the fourth intersection in urban environments (Figure 8), in suburban environments the vehicle idles for 30 s at the first intersection and for 2 s at the fourth intersection (Figure 9).

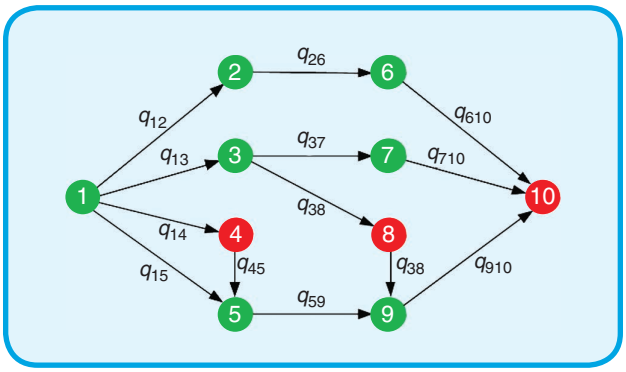


**FIG 7** A directed network graph.

Table 2. The distance and green/red time duration in urban environments.

| Intersection Number | Green Light Duration (s) | Red Light Duration (s) | Distance Between Two Intersections (m) | |
|---|---|---|---|---|
| | | | Urban | Suburban |
| 1 | 20 | 30 | 600 | 1,000 |
| 2 | 30 | 40 | 700 | 1,100 |
| 3 | 60 | 70 | 600 | 1,200 |
| 4 | 40 | 60 | 1,000 | 1,100 |
| 5 | 50 | 70 | 800 | 1,500 |
| 6 | 0 | +∞ | 1,000 | 1,200 |

In suburban environments, at the first intersection, the vehicle decelerates to 0 m/s first and then accelerates to 23.0 m/s under the variable speed driving strategy. The speed profile is continuous at all intersections. However, this feature cannot be guaranteed by the constant speed driving strategy. We can see that at the fourth intersection, the velocity suddenly jumps from 22.9 m/s directly to 25.8 m/s. The step–change speed of the constant speed driving strategy indicates that this driving strategy is less accurate and cannot be applied in reality. In contrast, the variable speed driving strategy, which considers the acceleration and deceleration process, is more realistic for actual vehicle control.

Table 3 presents the comparison of the fuel consumption results between the variable speed driving strategy and constant speed driving strategy in both environments. Compared to the constant speed driving strategy, the variable speed driving strategy saves 9.87% of the fuel, albeit with a 15.76% increase in travel time in urban environments. Similarly, although the variable speed driving strategy consumes more travel time (60.47%), it saves 3.8% of the fuel in suburban environments. We emphasize that the

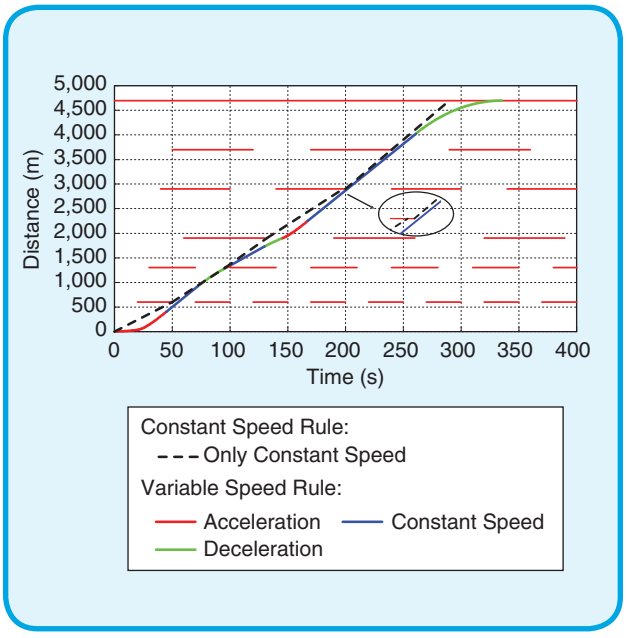


**FIG 8** The traveling trajectories of the variable speed and constant speed driving strategies in urban environments.

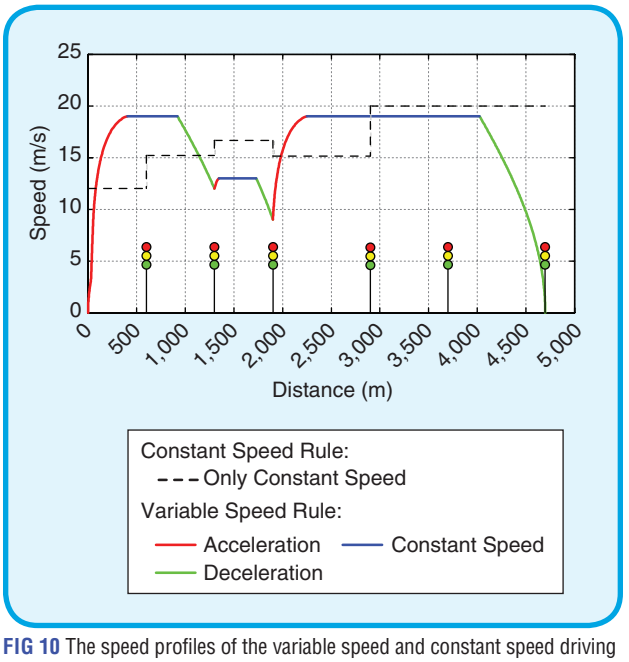


**FIG 10** The speed profiles of the variable speed and constant speed driving strategies in urban environments.

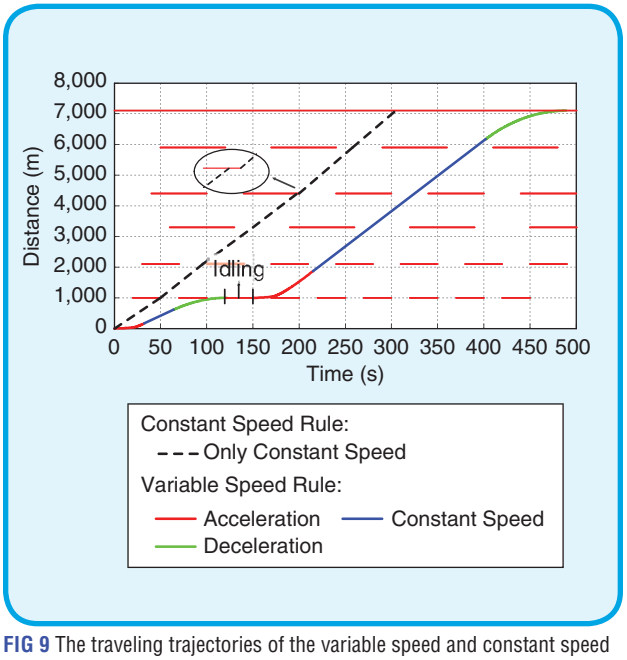


**FIG 9** The traveling trajectories of the variable speed and constant speed driving strategies in suburban environments.

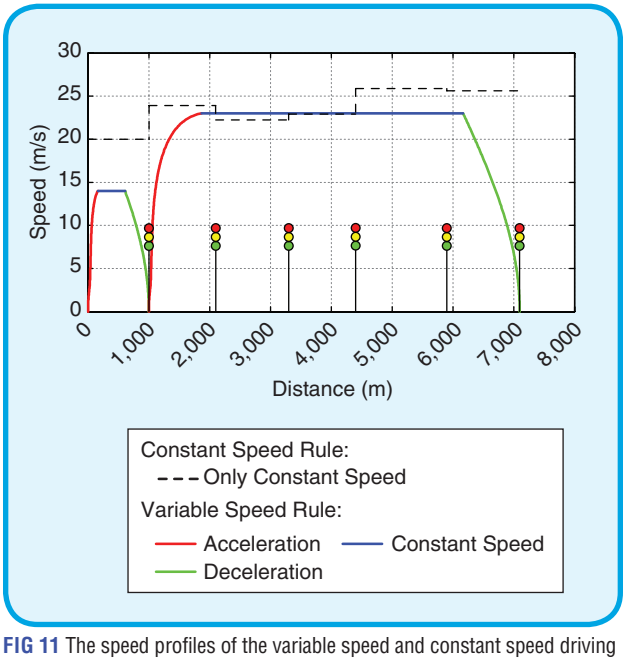


**FIG 11** The speed profiles of the variable speed and constant speed driving strategies in suburban environments.

constant speed driving strategy does not consider the acceleration and deceleration during the traveling process. The lack of acceleration and deceleration reduced the travel time in the simulation, and the real travel time and fuel consumption must be higher than the simulated values.

### *Simulation With a Different Setting*

In this section, we modified the traffic phases slightly to show the fuel economy. The changes are listed here:

- In the urban environments, the end time of the second red light at the fourth intersection is reduced from 200 to 190 s; that is, the time duration of the red light is changed from 60 to 50 s, shown as the dashed red circle in Figure 12.
- In the suburban environments, the third red light time duration at the first intersection, the third red light time duration at the fourth intersection, and the second red light time duration at the third intersection are changed

Table 3. The comparison of fuel consumption results between the variable speed driving strategy and constant speed driving strategy.

| Driving Strategy Type | Fuel Consumption (g) | | Travel Time (s) | |
|---|---|---|---|---|
| | Urban | Suburban | Urban | Suburban |
| Constant speed | 419.68 | 572.88 | 290.00 | 304.88 |
| Variable speed | 378.27 | 551.09 | 335.69 | 489.24 |
| Comparison | –9.87% | –3.80% | 15.76% | 60.47% |

from 30 to 10 s, from 60 to 50 s, and from 70 to 50 s, respectively.

Figures 12 and 13 demonstrate the new traveling trajectories; Figures 14 and 15 present the new vehicle speed profiles. With Change 1 as indicated by the red dashed circle in Figure 12, there is no longer any idling time. With Change 2 as indicated by the red dashed circles in Figure 13, the related lasting idling can also be removed.

Table 4 presents the comparison of the new fuel consumption results with the changed traffic light settings. In the urban scenario, the variable speed driving strategy consumes 14.50% more travel time and saves 10.14% of the fuel, whereas the two values were 15.76 and –9.87% in the original setting. Similarly, in the suburban environments, compared to the constant speed driving strategy, the variable speed driving strategy consumes 55.67% more travel time and saves 5.04% of the fuel, changed from 60.47 and –3.80%. Based on these results, we can find that the different driving strategies' performance may change a lot under different traffic phase settings.

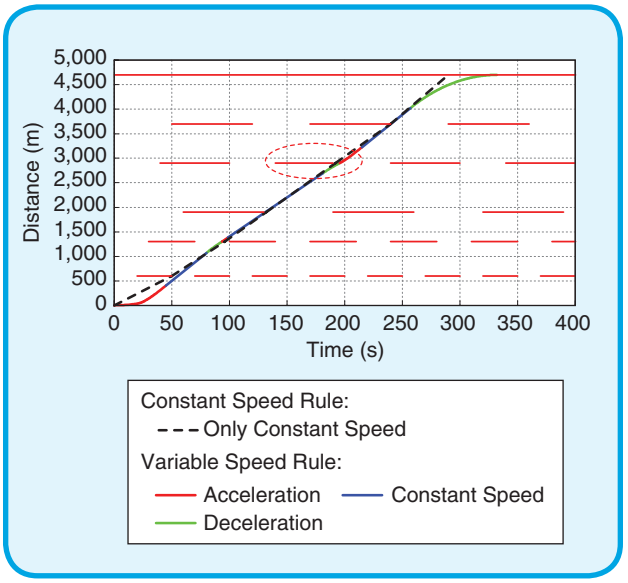


**FIG 12** The traveling trajectories of the variable speed and constant speed driving strategies with changed time duration of the red light in urban environments.

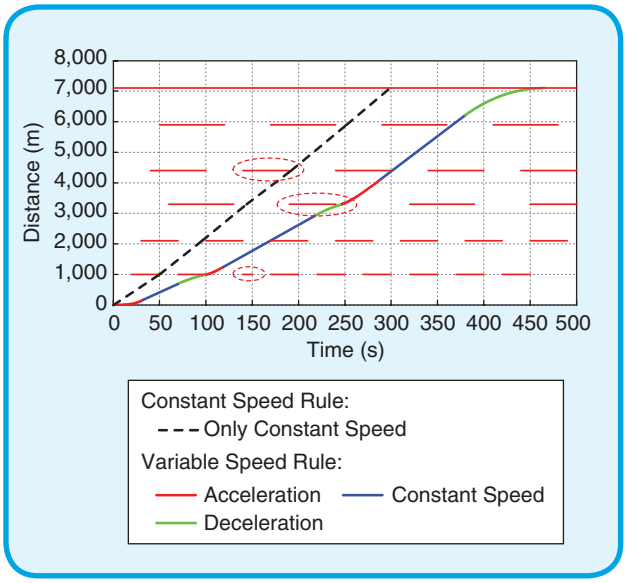


**FIG 13** The traveling trajectories of the variable speed and constant speed driving strategies with changed time duration of the red light in suburban environments.

## Conclusions

This article studied the fuel-saving operation for a vehicle passing through multiple signalized intersections. The open-loop optimal control problem that describes a vehicle traveling between two red-signalized intersections was formulated first and then numerically solved by the Legendre pseudospectral technique. The two- or three-stage operation rule was proposed to approximate the numerical solutions for fast computation. The fuel-saving operation for multiple intersections was solved by combining the two- or three-stage operation rule and the Dijkstra algorithm. Simulation results demonstrate that compared to the constant speed driving strategy, this method can save more fuel and create more realistic instantaneous speed changes when the vehicle passes through multiple signalized intersections. Practical applications of the findings may include automatic drive systems and some fuel-oriented driving assistance systems.

The present study can be extended to more research directions. One typical topic is the eco-driving strategy design for a fleet rather than for a single vehicle, which may improve the systematic fuel efficiency. Another potential topic is the optimization of a mixed fleet with a certain penetration rate of CAVs. The eco-driving strategies, designed for an individual vehicle or a fleet of vehicles, may have a negative impact on the overall operational efficiency of the intersection in terms of travel delays and increased overall fuel consumption. For example, an Eco-CACC algorithm-considering queue is developed, and the results show that for single-lane approaches, the algorithm reduces the overall fuel consumption levels for all vehicles and that higher market penetration rates (MPRs)

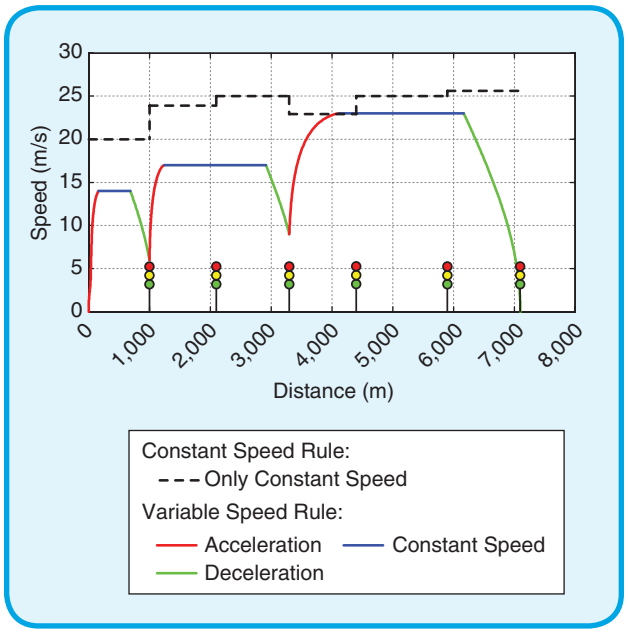


**FIG 14** The speed profiles of the variable speed and constant speed driving strategies with changed time duration of the red light in urban environments.

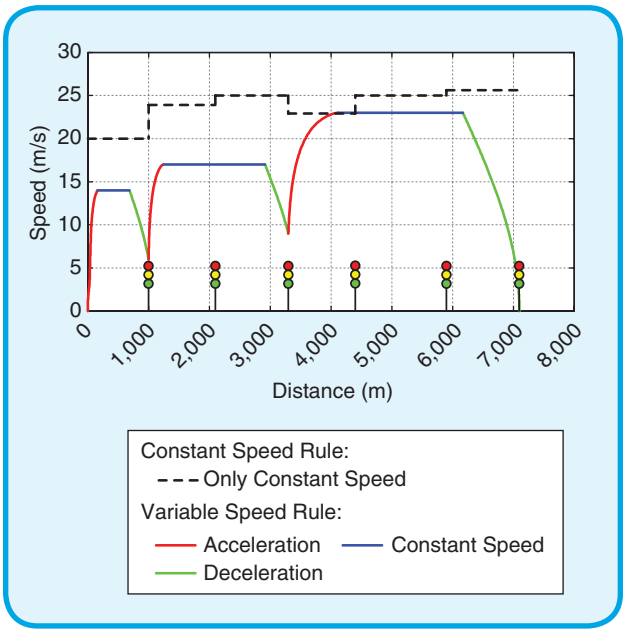


**FIG 15** The speed profiles of the variable speed and constant speed driving strategies with changed time duration of the red light in suburban environments.

Table 4. The comparison of fuel consumption results with changed red light between the variable speed driving strategy and constant speed driving strategy.

| Driving Strategy Type | Fuel Consumption (g) | | Travel Time (s) | |
|---|---|---|---|---|
| | Urban | Suburban | Urban | Suburban |
| Constant speed | 415.93 | 573.15 | 290.00 | 298.88 |
| Variable speed | 373.76 | 544.25 | 332.06 | 465.25 |
| Comparison | –10.14% | –5.04% | 14.50% | 55.67% |

result in larger savings, whereas on multilane approaches, lower MPRs have negative impacts on the overall intersection fuel efficiency [18]. Thus, how to adapt the proposed strategies to real traffic conditions, particularly in a mixed traffic flow, is key to field implementation. Two aspects of future work are envisaged as follows: One is to examine how the key parameters of the proposed strategy, e.g., the minimum spacing between vehicles, speed limit, and the parameters of the car-following model will affect the traffic flow as a whole. The other is the impact of the MPRs of CAVs deployed with eco-driving strategies. In addition, the vehicle fleets with an automated leader or with a human-operated leader should also be analyzed.

## Acknowledgments

This study is supported by the National Key R&D Program of China (2017YFB0102603). Special thanks should be given to Toyota for partially funding this study. Shengbo Eben Li and Qingfeng Lin contributed equally to this work. The corresponding authors of this article are Shengbo Eben Li and Qingfeng Lin.

## About the Authors

***Qingfeng Lin*** (linqf@buaa.edu.cn) earned his M.S. and Ph.D. degrees in vehicle operation engineering from Jilin University, Changchun, China, in 2003 and 2006. He is currently an assistant professor with the School of Transportation Science and Engineering, Beihang University, China. During 2006–2008, he was a postdoctoral researcher at the Tsinghua University, Beijing. His research work mainly focus on intelligent vehicle and driver behavior.

***Shengbo Eben Li*** (lisb04@gmail.com) earned his M.S. and Ph.D. degrees from Tsinghua University, Beijing, in 2006 and 2009. He is currently a tenured associate professor at Tsinghua University. His active research interests include intelligent vehicles and driver assistance, reinforcement learning and distributed control, optimal control and estimation, and so forth. He is the author of more than 100 peer-reviewed journal/conference papers and the coinventor of more than 20 Chinese patents. He was the recipient of the Best Paper Award in the 2014 IEEE ITS Symposium, the Best Paper Award in the 14th ITS Asia Pacific Forum, the National Award for Technological Invention in China (2013), the Excellent Young

Scholar of NSF China (2016), and the Young Professorship of Changjiang Scholar Program (2016).

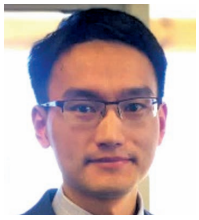

***Shaobing Xu*** (xushao@umich.edu) received his Ph.D. degree in mechanical engineering from Tsinghua University, Beijing, China, in 2016. He is currently an assistant research scientist with the Department of Mechanical Engineering and Mcity at the University of Michigan, Ann Arbor. His research focuses on vehicle motion control, decision making, and path planning for autonomous vehicles. He was a recipient of the outstanding Ph.D. dissertation award of Tsinghua University and the Best Paper Award of AVEC'2018.

***Xuejin Du*** (15201316042@163.com) earned her B.S. degree in traffic engineering from Beijing Jiaotong University in 2014 and her M.S. degree in traffic engineering from Beihang University, Beijing, in 2017. She is currently a researcher with the Commercial Vehicle Technology Center of SAIC, Shanghai, in China. Her research interests include optimal control theory and vehicle dynamics control.

***Diange Yang*** (ydg@tsinghua.edu.cn) earned his B.S. and Ph.D. degrees in automotive engineering from Tsinghua University, Beijing, in 1996 and 2001, respectively. He is a professor at the Department of Automotive Engineering of Tsinghua University. His research work mainly focus on intelligent vehicle and autonomous driving. He has received numerous awards during his career, including the Distinguished Young Science Technology talent of Chinese Automobile Industry in 2011 and the Excellent Young Scientist of Beijing in 2010. He was also the recipient of the Second Prize of National Technology Invention Rewards of CHINA in 2010 and in 2013.

***Keqiang Li*** (likq@tsinghua.edu.cn) earned his M.S. and Ph.D. degrees from Chongqing University, China, in 1988 and 1995, respectively, and his B.Tech degree from Tsinghua University in 1985. He is a professor of automotive engineering at Tsinghua University. His main research areas include intelligent and connected vehicles, automotive control and driver assistance systems, vehicle dynamics, and control. Currently, he is leading the national key project on connected and automated vehicles in China.

## References


[1] S. E. Li, S. Xu, X. Huang, B. Cheng, and H. Peng, "Eco-departure of connected vehicles with V2X communication at signalized intersections," *IEEE Trans. Veh. Technol.*, vol. 64, no. 12, pp. 5439–5449, Dec. 2015. doi: 10.1109/TVT.2015.2483779.

[2] M. J. M. Sullman, L. Dorn, and P. Niemi, "Eco-driving training of professional bus drivers: Does it work?" *Transp. Res. C, Emerg. Technol.*, vol. 58, part D, pp. 749–759, Sept. 2015. doi: 10.1016/j.trc.2015.04.010.

[3] S. L. Jamson, D. L. Hibberd, and A. H. Jamson, "Drivers' ability to learn eco-driving skills; effects on fuel efficient and safe driving behaviour," *Transp. Res. C, Emerg. Technol.*, vol. 58, part D, pp. 657–668, Sept. 2015. doi: 10.1016/j.trc.2015.02.004.

[4] A. Zavalko, "Applying energy approach in the evaluation of eco-driving skill and eco-driving training of truck drivers," *Transp. Res. D, Transp. Environ.*, vol. 62, pp. 672–684, July 2018. doi: 10.1016/j.trd.2018.01.023.

[5] Y. Wu, X. Zhao, J. Rong, and Y. Zhang, "The effectiveness of eco-driving training for male professional and non-professional drivers," *Transp. Res. D, Transp. Environ.*, vol. 59, pp. 121–133, Mar. 2018. doi: 10.1016/j.trd.2018.01.002.

[6] M. Zarkadoula, G. Zoidis, and E. Tritopoulou, "Training urban bus drivers to promote smart driving: A note on a Greek eco-driving pilot program," *Transp. Res. D, Transp. Environ.*, vol. 12, no. 6, pp. 449–451, Aug. 2007. doi: 10.1016/j.trd.2007.05.002.

[7] B. Beusen et al., "Using on-board logging devices to study the longer-term impact of an eco-driving course," *Transp. Res. D, Transp. Environ.*, vol. 14, no. 7, pp. 514–520, Oct. 2009. doi: 10.1016/j.trd.2009.05.009.

[8] W. Liu, Y. Yin, and H. Yang, "Effectiveness of variable speed limits considering commuters' long-term response," *Transp. Res. B, Methodol.*, vol. 81, part 2, pp. 498–519, Nov. 2015. doi: 10.1016/j.trb.2014.12.001.

[9] S. E. Li and H. Peng, "Strategies to minimize the fuel consumption of passenger cars during car-following scenarios," in *Proc. Inst. Mech. Eng., D, J. Automob. Eng.*, vol. 226, no. 3, pp. 419–429, Mar. 2012. doi: 10.1177/0954407011420214.

[10] S. E. Li, H. Peng, K. Li, and J. Wang, "Minimum fuel control strategy in automated car-following scenarios," *IEEE Trans. Veh. Technol.*, vol. 61, no. 3, pp. 998–1007, Jan. 2012. doi: 10.1109/TVT.2012.2183401.

[11] S. E. Li, X. Hu, K. Li, and C. Ahn, "Mechanism of vehicular periodic operation for optimal fuel economy in free-driving scenario," *IET Intell. Transp. Syst.*, vol. 9, no. 3, pp. 306–313, Mar. 2015. doi: 10.1049/iet-its.2014.0002.

[12] S. Sato, H. Suzuki, M. Miya, and N. Lida, "Analysis of the effect of eco-driving with early shift-up on real-world emission," SAE Technical Paper, 2010-01-2279, 2010.

[13] G. Thomas and P. G. Voulgaris, "Fuel minimization of a moving vehicle in suburban traffic," in *Proc. 2013 American Control Conf.*, Washington, D.C., pp. 4009–4014. doi: 10.1109/ACC.2013.6580453.

[14] G. De Nunzio, C. C. De Wit, P. Moulin, and D. Di Domenico, "Eco-driving in urban traffic networks using traffic signal information," in *Proc. 52nd IEEE Conf. Decision and Control*, Florence, Italy, Dec. 10–13, 2013, pp. 892–898. doi: 10.1109/CDC.2013.6759995.

[15] R. K. Kamalanathsharma and H. A. Rakha, "Multi-stage dynamic programming algorithm for eco-speed control at traffic signalized intersections," in *Proc. 16th IEEE Conf. Intelligent Transportation Systems*, The Hague, The Netherlands, Oct. 6–9, 2013, pp. 2094–2099. doi: 10.1109/ITSC.2013.6728538.

[16] R. K. Kamalanathsharma and H. A. Rakha, "Leveraging connected vehicle technology and telematics to enhance vehicle fuel efficiency in the vicinity of signalized intersections," *J. Intell. Transp. Syst.*, vol. 20, no. 1, pp. 33–44, 2016. doi: 10.1080/15472450.2014.889916.

[17] R. K. Kamalanathsharma, H. A. Rakha, and H. Yang, "Networkwide impacts of vehicle ecospeed control in the vicinity of traffic signalized intersections," *Transp. Res. Rec., J. Transp. Res. Board*, vol. 2503, no. 1, pp. 91–99, 2015. doi: 10.3141/2503-10.

[18] H. Yang, H. Rakha, and M. V. Ala, "Eco-cooperative adaptive cruise control at signalized intersections considering queue effects," *IEEE Trans. Intell. Transp. Syst.*, vol. 18, no. 6, pp. 1575–1585, 2017. doi: 10.1109/TITS.2016.2613740.

[19] X. Zeng and J. Wang, "Globally energy-optimal speed planning for road vehicles on a given route," *Transp. Res. C, Emerg. Technol.*, vol. 93, pp. 148–160, Aug. 2018. doi: 10.1016/j.trc.2018.05.027.

[20] P. Schuricht, O. Michler, and B. Baker, "Efficiency-increasing driver assistance at signalized intersections using predictive traffic state estimation," in *Proc. 14th IEEE Conf. Intelligent Transportation Systems (ITSC)*, Washington, D.C., Oct. 5–7, 2011, pp. 347–352. doi: 10.1109/ITSC.2011.6083111.

[21] H. Xia, K. Boriboonsomsin, and M. Barth, "Dynamic eco-driving for signalized arterial corridors and its indirect network-wide energy/emissions benefits," *J. Intell. Transp. Syst. Technol. Plann. Oper.*, vol. 17, no. 1, pp. 31–41, 2013. doi: 10.1080/15472450.2012.712494.

[22] J. Sun, D. Niu, S. Chen, and K. Li, "Development and investigation of a dynamic eco-driving speed guidance strategy for signalized highway traffic," in *Proc. 92nd Annu. Meeting Transportation Research Board*, Washington, D.C., 2013.

[23] N. Wan, A. Vahidi, and A. Luckow, "Optimal speed advisory for connected vehicles in arterial roads and the impact on mixed traffic," *Transp. Res. C, Emerg. Technol.*, vol. 69, pp. 548–563, Aug. 2016. doi: 10.1016/j.trc.2016.01.011.

[24] T. Q. Tang, Z. Y. Yi, J. Zhang, and N. Zheng, "Modelling the driving behaviour at a signalised intersection with the information of remaining green time," *IET Intell. Transport Syst.*, vol. 11, no. 9, pp. 596–603, 2017. doi: 10.1049/iet-its.2017.0191.

[25] E. Ozatay, U. Ozguner, S. Onori, and G. Rizzoni, "Analytical solution to the minimum fuel consumption optimization problem with the existence of a traffic light," in *Proc. ASME 5th Dynamic Systems and Control Conf. Joint with JSME Motion and Vibration*, Fort Lauderdale, FL, Oct. 17–19, 2012, pp. 837–846. doi: 10.1115/DSCC2012-MOVIC2012-8535.

[26] Q. Lin, X. Du, S. E. Li, and Z. Ye, "Vehicle-to-infrastructure communication based eco-driving operation at multiple signalized intersections," in *Proc. 13th IEEE Vehicle Power and Propulsion Conf. (VPPC)*, Hangzhou, China, Oct. 17–20, 2016, pp. 102–107. doi: 10.1109/VPPC.2016.7791809.

[27] Q. Lin et al., "Minimize the fuel consumption of connected vehicles between two red-signalized intersections in urban traffic," *IEEE Trans. Veh. Technol.*, vol. 67, no. 10, pp. 9060–9072, Aug. 2018. doi: 10.1109/TVT.2018.2864616.

[28] S. Xu, S. E. Li, K. Deng, S. Li, and B. Cheng, "A unified pseudospectral computational framework for optimal control of road vehicles," *IEEE/ASME Trans. Mechatronics*, vol. 20, no. 4, pp. 1499–1510, Aug. 2015. doi: 10.1109/TMECH.2014.2360613.

[29] S. E. Li, S. Xu, and D. Kum, "Efficient and accurate computation of model predictive control using pseudospectral discretization," *Neurocomputing*, vol. 177, pp. 363–372, Feb. 2016. doi: 10.1016/j.neucom.2015.11.020.

[30] F. Fahroo and I. M. Ross, "Advances in pseudospectral methods for optimal control," presented at the AIAA Guidance, Navigation and Control Conf. and Exhibit, Honolulu, HI, Aug. 18–21, 2008, AIAA paper 2008-7309. doi: 10.2514/6.2008-7309.

[31] P. E. Gill, W. Murray, and M. A. Saunders, "SNOPT: An SQP algorithm for large-scale constrained optimization," *SIAM Rev.*, vol. 47, no. 1, pp. 99–131, Jan. 2005. doi: 10.1137/S0036144504446096.

[32] Q. Jin, G. Wu, K. Boriboonsomsin, and M. J. Barth, "Power-based optimal longitudinal control for a connected eco-driving system," *IEEE Trans. Intell. Transp. Syst.*, vol. 17, no. 10, pp. 2900–2910, Oct. 2016. doi: 10.1109/TITS.2016.2535439.

ITS